

Effect of purity on the properties of ultrafine HNS

Wenzheng Xu*, Chongwei An*[†], and Jingyu Wang*

*Chemical Industry and Ecology Institute, North University of China, Taiyuan, Shanxi 030051 CHINA

TEL : +86 03513922140

[†]Corresponding address : acw98081b1@163.com

Received : August 3, 2011 Accepted : September 29, 2011

Abstract

Two ultrafine HNS particles with different purity were prepared by Laval nozzle assisted precipitation method. SEM (Scanning Electron Microscope), laser granularity measurement, high performance liquid chromatograph (HPLC), dynamic contact angle measurement and X-ray diffraction (XRD) were employed to characterize the ultrafine HNS samples. The filtration speed, impact sensitivity, short pulse shockwave sensitivity and thermal stability of the two ultrafine HNS particles were also studied and contrasted. Results show that the two ultrafine HNS samples have the similar particle size, morphology and crystal type. However, the sample with higher purity has higher surface energy and lower Zeta potential, which results in the higher filtration speed. Both impact and short duration shock sensitivity of ultrafine raw HNS are lower than those of ultrafine purified HNS. Moreover, compared with ultrafine raw HNS, the thermal decomposition peak temperatures of ultrafine purified HNS at different heating rates decrease slightly, the activation energy hardly varies.

Keywords : ultrafine HNS, purity, properties

1. Introduction

2,2', 4,4', 6,6'-Hexanitrostilbene, also known as HNS or JD-X, is sufficiently insensitive to heat, impact, and electrostatic spark to be used in petroleum production and military ordnance systems¹. With the acceptable detonation velocity and sensitivity, it is used as an end booster explosive^{2,3}. According to the US military specification, HNS has multiple classifications such as HNS-I, HNS-II, and HNS-IV etc.. HNS-IV is a ultrafine-sized material with a surface area of 5.0 to 25.0 m²·g⁻¹, which is crash-precipitated from HNS-II that is recrystallized from HNS-I^{4,5}. The ultrafine HNS has been the explosive of choice for Exploding Foil Initiators (EFI), also called a slapper detonator due to the high short duration shock sensitivity⁶. It has been reported that HNS-I synthesized by a "one-step" process from trinitrotoluene (TNT) contains 5–10% impurities, such as hexanitrobenzyl (HNBB) or dipicrylethane (DPE)^{7–10}, which influences the explosive properties more or less. Although the MIL-E-82903 has established the purity requirements for ultrafine HNS, little research into the dependence of purity on the properties has been done. Herein, two ultrafine HNS particles with different purity were prepared by Laval

nozzle assisted precipitation method, and the particle size, morphology, crystal type, Zeta potential, surface energy, filtration speed, impact sensitivity, short pulse shockwave sensitivity and thermal stability of the two samples were investigated and contrasted in detail.

2. Experimental

2.1 Materials

Raw HNS was synthesized by the reported process and was certified to be with 95% chemical purity using HPLC. Dimethylformamide (C.P.), methyl alcohol (C.P.), and 1,4-dioxane (C.P.) were purchased from Tianjin Tianda chemicals Co., Ltd. Purified water was prepared in our own lab.

2.2 Methods

2.2.1 Purification of HNS

The purification of HNS was carried out by recrystallization process. HNS (10g) was dissolved in DMF (100 ml) at 150°C in the oil bath during 1.5 hrs. And then the solution was cooled below zero in the refrigerator. The solid was filtered off, washed with dioxane-MeOH (1 : 4 by volume, 2×10 ml) and purified water (2×15 ml). After

evaporation in vacuum at 65°C, the high purity HNS was obtained.

2.2.2 Preparation of ultrafine HNS particles

In this experiment, ultrafine raw HNS (UR-HNS) and ultrafine purified HNS (UP-HNS) were prepared by Laval nozzle assisted precipitation method at the same conditions. The experimental setup and the structure of nozzle were shown in Fig. 1. The preparation steps were as follows: raw (or purified) HNS was added into DMF at 70°C. After complete dissolution, the solution was filtered to remove insoluble impurities. When the purified water was pumped through the nozzle, the subatmospheric pressure was produced at the throat of nozzle. The solution was drawn into the nozzle and mixed rapidly with the water stream. By rapid precipitation, a yellow suspension was obtained. The suspension was filtered by a pressure filter at 0.4 MPa. The filtration cakes were washed with dioxan-MeOH and purified water to remove residual solvent. After freeze-dried the filter cake, the dried ultrafine HNS powders were obtained.

2.2.3 Characterization of ultrafine particles

The profiles and size of HNS-IV particles are characterized by S-4700 Scanning Electronic Microscope made by Hitachi Corporation, Japan. Particle size distribution and Zeta potential of ultrafine HNS particles are also measured with a BI-90PLUS laser particle sizer made by Brookhaven Instruments Corporation, USA. The X-ray diffraction (XRD) was carried out on a Rigaku D/MAX2550 VB+/PC (Japan) to distinguish the crystal type of sample. Chemical purity of HNS was analyzed by HP 1100 (USA) high performance liquid chromatograph (HPLC) according to MIL-E-82903 (OS). Surface energy of HNS particles is measured by DCAT 21 dynamic contact angle tester (Germany).

The DSC experiments are carried out with DSC131 instrument made by Setaram Co., France. The conditions of DSC are as follows: sample mass, 0.7 mg; heating rate, 5, 10, 20°C·min⁻¹; N₂ atmosphere (30 mL·min⁻¹). Impact sensitivity is surveyed by a 12 type drop hammer apparatus using an up-and-down method. The testing conditions are: drop weight, 2 kg; sample mass, 30 mg. They are expressed by the critical drop-height of 50% explosion probability (H_{50}) and standard deviation (S). The short duration shock initiation sensitivity of the compound was determined by the method of electrically exploded metal foil-driven flyer plate developed in our laboratory. The testing conditions are: voltage, 1800V; capacitance, 0.2 μF; polyimide flyer plate, 25 μm.

3. Results and discussions

3.1 Chemical purity analysis

The chemical purity of HNS samples are determined by HPLC analysis and the results are tabulated in Table 1.

The data in Table 1 indicate that the purity of HNS is increased from 95.07 wt.% to 99.62 wt.% by purification. Moreover, the purity of UR-HNS and UP-HNS are 94.98 wt.% and 99.31 wt.% respectively, which is lower than that of the corresponding raw sample. It is due to the fact that DMF residual solvent was introduced into the product in the ultrafine process.

3.2 Particle size and morphology

From Fig. 2, it can be seen that the mean diameter of

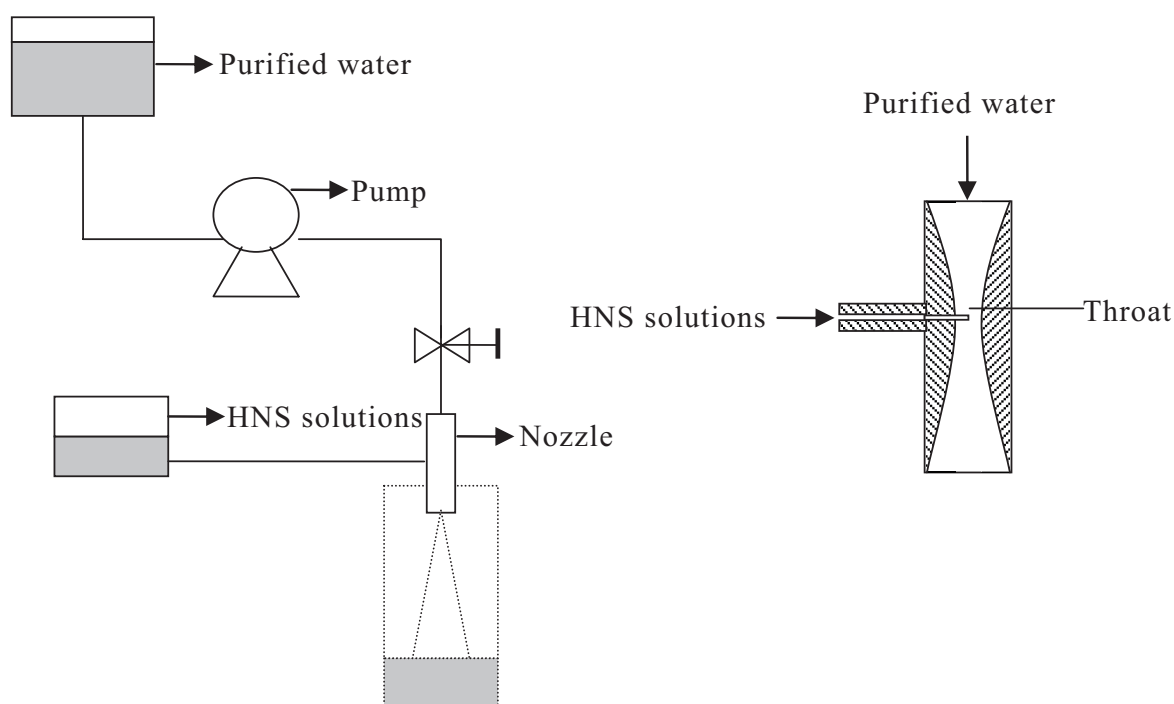


Fig. 1 Experimental setup for preparation of ultrafine HNS (left) and Structure of nozzle (right).

Table 1 Chemical purity of HNS samples.

Samples	Raw HNS	Purified HNS	UR-HNS	UP-HNS
Chemical purity[%]	95.07	99.62	94.98	99.31

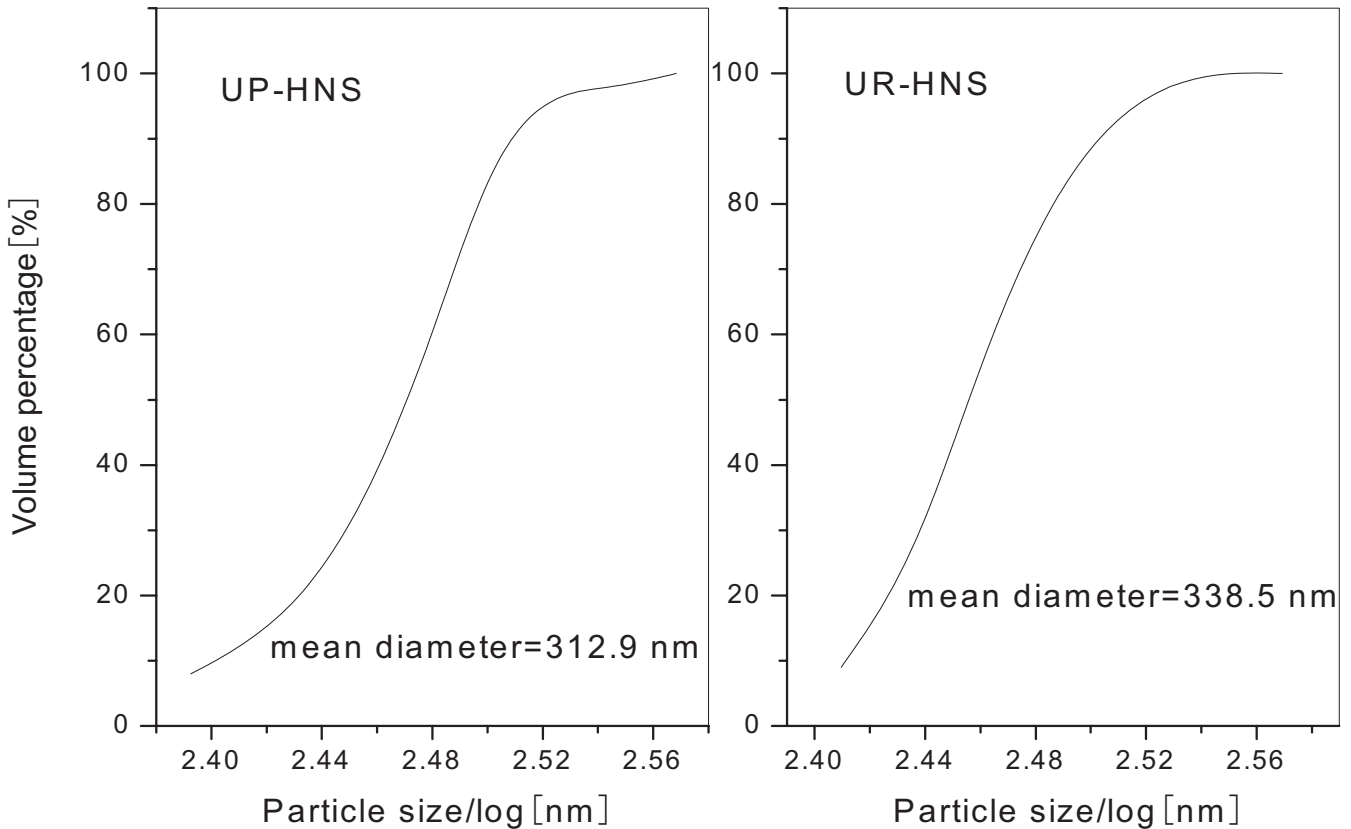


Fig. 2 Particle size distribution of UR-HNS and UP-HNS.

ultrafine raw and purified HNS are 338.5 nm and 312.9 nm respectively. The two size distribution curves are almost similar in shape and range, which indicates that two ultrafine particles have the same size distribution. Figure.3 shows that both ultrafine particles have the appearance of rodlike and their particle sizes range from 200–400 nm. The results indicate that the purity has no influence on the particle size and morphology of ultrafine HNS in the ultrafine process.

3.3 Crystal type

The X-ray diffraction spectra of raw and two ultrafine HNS samples are shown in Fig. 4.

It can be seen in Fig. 4 that the peaks of two ultrafine HNS samples have the peaks at the same diffraction angles, implying that the chemical purity does not change the crystal structure of HNS. Moreover, the peak intensity of ultrafine HNS samples are much weaker and wider than that of raw HNS. It is consistent with the fact that the X-ray peak will weaken or disappear with the grain size decreasing.

3.4 Zeta potential

Zeta potential is the electrical potential that exists at the shear plane of a particle, which is a function of the surface charge of a particle. Generally, the greater the absolute value of Zeta potential is, the better the dispersion of particles is. As is shown in Table 2, Zeta potential of UR-HNS and UP-HNS are 47.24 mv and 18.54 mv respectively, indicating that the ultrafine HNS particles with higher chemical purity have the better dispersion.

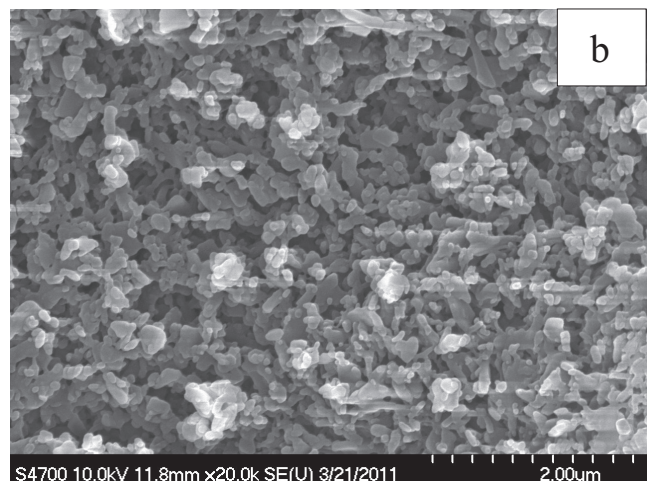
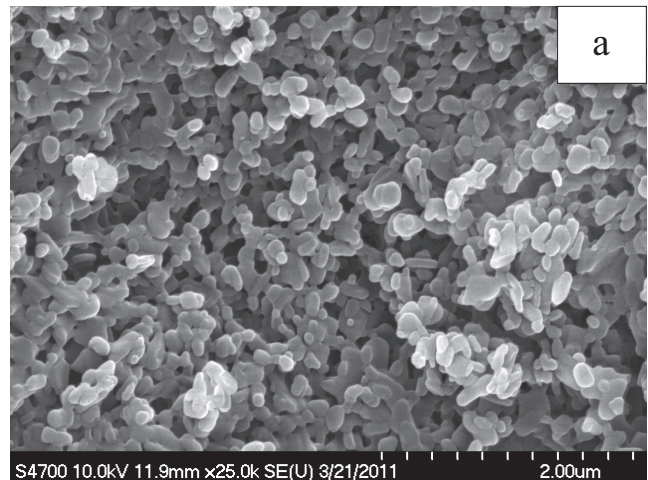


Fig. 3 SEM images of UR-HNS and UP-HNS, a : UR-HNS ; b : UP-HNS.

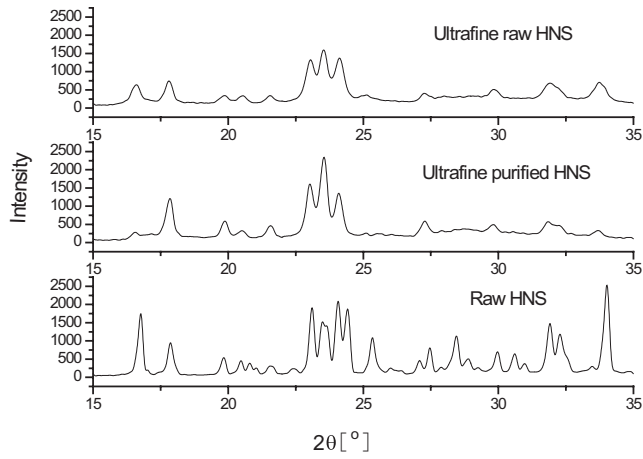


Fig. 4 X-ray diffraction spectra of raw and ultrafine HNS.

Table 2 Zeta potential and surface energy of UR-HNS and UP-HNS.

Samples	Max value [mv]	Average value [mv]	Surface energy [$\text{mJ}\cdot\text{m}^{-2}$]
UR-HNS	-71.72	-47.24	24.26
UP-HNS	-39.63	-18.54	34.52

3.5 Surface energy

The surface energy of UR-HNS and UP-HNS is tested by using dynamic contact angle method and the results are shown in Table 2. Table 2 shows that the surface energy of UR-HNS and UP-HNS are $24.26 \text{ mJ}\cdot\text{m}^{-2}$ and $34.52 \text{ mJ}\cdot\text{m}^{-2}$, respectively. It indicates that the ultrafine HNS with the higher purity has the higher surface energy.

3.6 Filtration velocity

UR-HNS and UP-HNS suspensions with the same solid content are filtered in the same conditions, and the plots of permeation velocity versus time for the two ultrafine HNS samples are shown in Fig. 5. Fig. 5 shows that in the filtration process, the permeation velocity of UR-HNS is much higher than that of UP-HNS. For the equal suspensions (3L), the filtration time of UR-HNS and UP-HNS is about 4 hour and 6 hour respectively. The fast filtration for UR-HNS is due to its higher Zeta potential and lower surface energy, which reduces the porosity of filter cake.

3.7 Impact sensitivity

The impact sensitivity results of UR-HNS and UP-HNS are summarized in Table 3. The data in Table 3 indicate that the critical drop height (H_{50}) of UP-HNS is 11.3cm lower than that of UR-HNS. It suggests that the HNS sample with higher chemical purity has the higher impact sensitivity.

3.8 Short duration shock sensitivity

Short duration shock sensitivity is a criterion to scale whether an explosive is used in EFI or not. The short duration shock initiation energy of UR-HNS and UP-HNS is 0.41 J and 0.26 J respectively. It indicates that UP-HNS

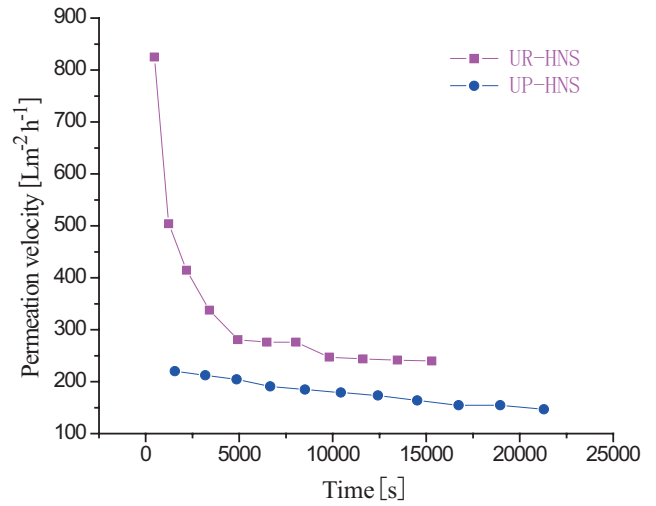


Fig. 5 Plots of permeation velocity versus time for the two ultrafine HNS samples.

Table 3 Impact sensitivity of UR-HNS and UP-HNS.

Samples	$H_{50}[\text{cm}]$				$\sigma[\text{cm}]$
	1	2	3	average	
UR-HNS	50.4	45.3	46.8	47.5	2.62
UP-HNS	32.0	37.6	38.9	36.2	3.67

has the higher short duration shock sensitivity and is more suitable for the charge of EFI.

3.9 Thermal stability

Figure 6 is the DSC curves of the two ultrafine HNS samples. In each case, the peak temperature and the peak area (decomposition heat) increase with increasing heating rate. At the same heating rate, the peak temperature of UP-HNS is slightly lower than that of UR-HNS. The Kissinger method (Equation 1)^(11,12) is used to acquire the activation energy of UR-HNS and UP-HNS, and the results are $176.02 \text{ kJ}\cdot\text{mol}^{-1}$ and $177.52 \text{ kJ}\cdot\text{mol}^{-1}$. It implies that the impurities of raw HNS have no effect on the thermal decomposition kinetics parameters of explosives.

$$\ln \frac{\beta_i}{T_i^2} = \ln \frac{AR}{E} - \frac{E}{RT_i} \quad (1)$$

Where E is the activation energy, $\text{kJ}\cdot\text{mol}^{-1}$, β_i is heating rate, $\text{K}\cdot\text{min}^{-1}$, T_i is the peak temperature of decomposition at β_i , K, A is the pre-exponential factor, R is the gas constant, $8.314 \text{ J}\cdot\text{mol}^{-1}\cdot\text{K}^{-1}$.

4. Conclusion

Two ultrafine HNS particles with different purity were prepared by Laval nozzle assisted precipitation method. The morphology, particle size, crystal type, Zeta potential, surface energy, filtration speed, impact sensitivity, short duration shock sensitivity and thermal stability of the two samples were investigated and contrasted extensively. Results show that purity has no effect on the particle size, morphology and crystal type of ultrafine HNS. However, the ultrafine HNS with higher purity has higher surface energy and lower Zeta potential, which results in the

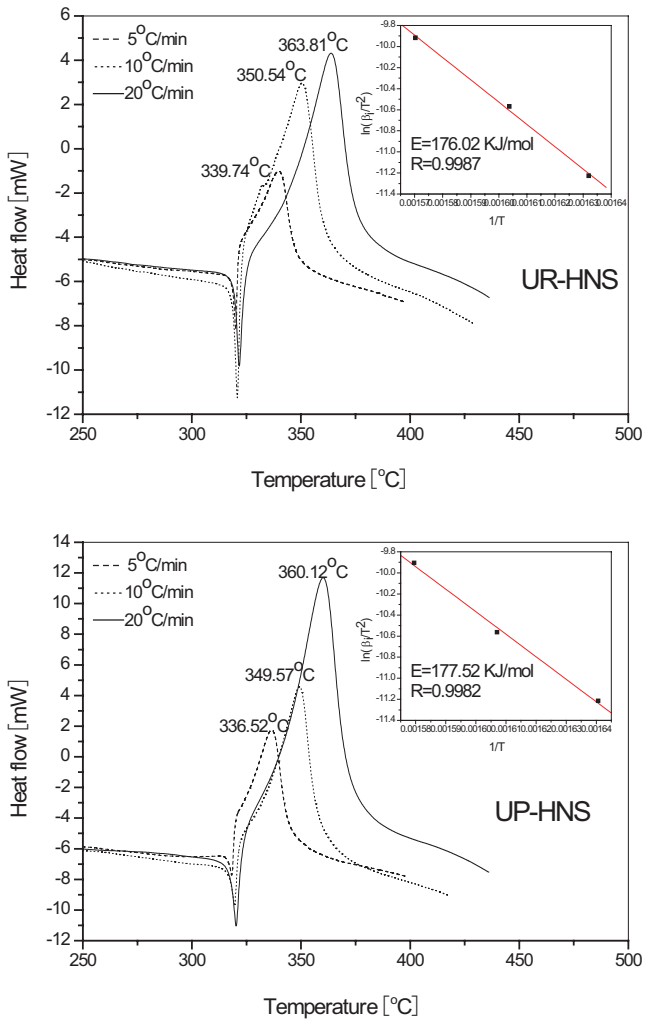


Fig. 6 DSC thermographs for ultrafine samples. Each inset is a Kissinger's plot for the thermal decomposition peak of the DSC curves. Symbol r is used to identify the linear coefficient of $\ln(\beta/T^2)$ to $1/T$.

lower filtration speed. Both impact and short duration shock sensitivity of ultrafine raw HNS are lower than that of ultrafine purified HNS. Moreover, compared with ultrafine raw HNS, the thermal decomposition peak temperature of ultrafine purified HNS at different heating rate decrease slightly, the activation energy hardly varies.

References

- 1) D. L. Williams and K. D. Kuklenz, *Propell. Explos. Pypot.*, 34, 452 (2009).
- 2) D. Cle'ment and K. P. Rudolf, *Propell. Explos. Pypot.*, 32, 322 (2007).
- 3) J. Waschl and D. Richardson, *J. Energ. Mater.*, 9, 269 (1991).
- 4) Navy MIL-E-82903, *Explosives HNS-IV and HNS-V*, Naval Surface Warfare Center, NAVSEA, Ordnance Systems (1999).
- 5) B.T. Neyer, L.Cox, T. Stoutenborough, and R. Tomasoski, 39th Joint Propulsion Conference and Exhibit, pp.1-6, Huntsville (2003).
- 6) S.M. Harris, S.E. Klassen, W.T. Quinlin, D.M. Cates, and R. Thorpe, *Proceedings of 41th AIAA Aerospace Sciences Meeting and Exhibit*, Reno, Nevada (2003).
- 7) A. J. Bellamy, *J. Energ. Mater.*, 28, 1(2010).
- 8) E. G. Kayser, *J. Energ. Mater.*, 1, 325 (1983).
- 9) A. J. Bellamy, T. P. Price, M. F. Mahon, R. Drake, and J. Mansell, *J. Energ. Mater.*, 23, 33 (2005).
- 10) A. Bellamy and E. Brzoska, *J. Energ. Mater.*, 21, 43 (2003).
- 11) R.Z.Hu, Z.Q.Yang, and Y.J.Liang, *Thermochim. Acta*, 134, 429 (1988).
- 12) C. W. An, X. D. Guo, X. L. Song, Y. Wang, and F. S. Li, *J. Energ. Mater.*, 27, 118 (2009).